

Perfect state transfer and maximal entanglement in a trimer of three-level systemsAbuenameh Aiyejina^{*,} Ethan Wyke^{†,} and Roger Andrews^{‡,}*Department of Physics, The University of the West Indies, St. Augustine, Trinidad and Tobago*Andrew D. Greentree[§]*ARC Centre of Excellence for Nanoscale BioPhotonics, School of Science, RMIT University, Melbourne, Victoria 3001, Australia*

(Received 26 May 2023; accepted 11 September 2023; published 25 September 2023)

We analyze a quantum wire that consists of a linear chain of three qutrits with nearest-neighbor interactions and detuning on the central qutrit. We derive the detuning conditions for perfect state transfer of a double excitation and for maximal entanglement between the first and third qutrits. We also analytically determine the times for perfect state transfer and maximal entanglement, which are found to be periodic. We also show that perfect state transfer is a necessary condition for maximal entanglement, with the first occurrence of maximal entanglement at half the time for the first occurrence of perfect state transfer.

DOI: [10.1103/PhysRevA.108.032421](https://doi.org/10.1103/PhysRevA.108.032421)**I. INTRODUCTION**

Quantum information science has emerged as one of the most critical technologies for the 21st century [1], fueling new concepts in physics and engineering, and forcing critical reappraisals of known results [2]. Classical information science is typically based around bits due to the robustness that arises from placing a threshold level between two distinguishable states. For example, with transistors, a threshold level between the current levels for on and off provides a natural form of error suppression. Although most quantum information technologies are based around qubits, i.e., the quantum analog of bits, in most quantum systems there is no analogy of classical thresholding, and most quantum systems can only be approximated as two-state systems.

Trimers, which are configurations (e.g., a linear chain) of three two-level systems (2LSs) or three-level systems (3LSs), have recently been studied by several authors. Trimers can exhibit perfect state transfer, which occurs when there is unit probability of finding the excitation on the end site of the trimer when starting with the excitation on the first site of the trimer. Bengtson and Sjöqvist [3] analyzed quantum coherence in a trimer of 2LSs. They found that in the trimer, the Hamiltonian parameters that give maximum coherence in the site basis are different from those that give perfect state transfer across the trimer. Wyke *et al.* [4] considered quantum excitation transfer and entanglement in a trimer of 2LSs with detuning on the second 2LS. They found that in the absence of a bath, the amplitude of the oscillations of the excitation probability does not change with the detuning on the second

2LS, whereas the presence of the detuning on the second 2LS increases the entanglement between the first and third 2LSs. Christandl *et al.* [5] examined a linear chain of 2LSs and showed that perfect state transfer along a chain of arbitrary length can be obtained by using suitably engineered couplings between the 2LSs without the need for any dynamical control.

Extending beyond qubits, d -dimensional quantum states are usually termed qudits, with three-state systems termed qutrits. Qutrits have certain advantages over qubit systems, motivating further investigation into systems that use them. Physical implementations of qutrits occur in several situations, including a spin-one particle in an external magnetic field, three states of an atom coupled by lasers, and some superconducting quantum circuits [6–8]. Such systems can have a Λ , V , or Ξ (also called ladder or cascade) energy level configuration. They exhibit phenomena such as electromagnetically induced transparency (EIT) [9], Autler-Townes splitting (ATS) [10], and stimulated Raman adiabatic passage (STIRAP) [11].

In certain systems, qutrits can optimize the available Hilbert space [12] and provide efficiency advantages over qubit-based systems [13–16]. Qutrits also offer advantages such as higher channel capacities and noise resilience in communication systems [17]. Recently, researchers have been successful in performing experiments with qutrits. Luo *et al.* [18] demonstrated quantum teleportation of a photonic qutrit with a fidelity of 75%. Senko *et al.* [19] experimentally realized a linear chain of qutrits with controllable interactions. They observed the time evolution of the system and entangled a pair of qutrits with 86% fidelity. We expect that these applications and advantages will also apply in solid-state systems which utilize quantum wires consisting of linear chains of qutrits, which forms the basis of this paper.

Gokhale *et al.* [16] showed that using qutrits instead of qubits significantly reduces the resources required for

*abuenameh.aiyejina@sta.uwi.edu

†ethan.wyke@my.uwi.edu

‡roger.andrews@sta.uwi.edu

§andrew.greentree@rmit.edu.au

quantum computations. They also demonstrated exponential improvements to the generalized Toffoli gate by using qutrits. Goss *et al.* [7] generated two universal two-qutrit gates with a measured process fidelity for a two-qutrit entangling gate of 97%. They were also able to establish a protocol for characterizing gate noise and determining the fidelity of gate operations.

Greentree and Koiller [20] demonstrated qutrit state transfer via dark state adiabatic passage in a chain of qutrits. Recently, Aiyejina *et al.* [21] demonstrated numerically near-perfect state transfer of a double excitation in a chain of three qutrits, in which the first qutrit is initially excited by a Gaussian laser pulse and there is a detuning on the second qutrit.

Perfect state transfer has important applications in quantum information processing. For example, in quantum communication and cryptography, entanglement is usually generated between an initial site and an end site of a communication channel. In solid-state systems, linear arrays of qubits or qutrits can act as quantum wires, which are the quantum information channels in devices and quantum networks. Perfect state transfer has already been analytically demonstrated in a quantum wire of qubits, where periodic perfect state transfer was obtained using specific interqubit interactions [5].

In this paper, we analytically investigate quantum excitation transfer and entanglement in a trimer of ladder-type 3LSs. In particular, we examine the transfer of a double excitation and we use the negativity as a measure of the entanglement between the first and third 3LSs. In Sec. II, we introduce the theory for the trimer Hamiltonian, and in Sec. III, we analytically solve the Hamiltonian and derive analytic expressions for the excitation probabilities and the negativity describing the entanglement between the first and third 3LSs. In Sec. IV, we derive analytic expressions for the detunings and times which give perfect state transfer and maximal entanglement. Finally, in Sec. V, we present simulations for the excitation probabilities and negativities for various detunings that either give perfect or imperfect state transfer.

II. THEORY

We examine a chain of three dipole-coupled 3LSs with ladder configurations having states $|0\rangle$, $|1\rangle$, and $|2\rangle$, as shown in Fig. 1. We include a detuning of the transition energies of the second 3LS with respect to the other two 3LSs. The Hamiltonian for this system is

$$H = \sum_{i=1}^3 (\omega S_{11}^i + 2\omega S_{22}^i) + \Delta S_{11}^2 + 2\Delta S_{22}^2 + J \sum_{i=1}^2 [(S_{01}^i + \sqrt{2}S_{12}^i)(S_{10}^{i+1} + \sqrt{2}S_{21}^{i+1}) + \text{H.c.}], \quad (1)$$

where ω is the energy separation of adjacent atomic levels for the first and third 3LSs, Δ is the detuning of the second 3LS, J is the dipole coupling strength of adjacent 3LSs, and $S_{nm}^i = |n\rangle_{ii}\langle m|$ is the operator for transitions from state $|m\rangle$ to state $|n\rangle$ of the i th 3LS. This Hamiltonian has been generalized from the Hamiltonian in Ref. [22] to allow for

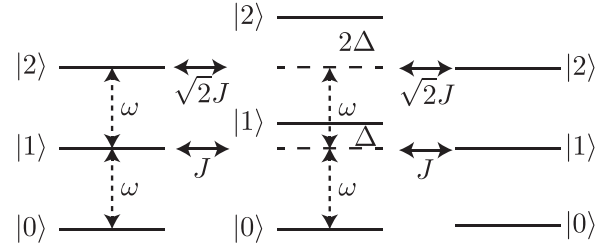


FIG. 1. Energy levels for the trimer system described by the Hamiltonian in Eq. (1). The energy levels of each 3LS are equally spaced, with the central 3LS detuned from the other two by Δ , as indicated. Excitations hop along the network with coupling constant J .

interatomic couplings that vary with the atomic transitions. In order to obtain analytic results, we have chosen the coupling for transitions involving the states $|0\rangle$ and $|1\rangle$ on both 3LSs to be J , and the coupling for transitions involving the states $|0\rangle$ and $|1\rangle$ on one 3LS and the states $|1\rangle$ and $|2\rangle$ on the other 3LS to be $\sqrt{2}J$. Finally, we have chosen the coupling for transitions involving the states $|1\rangle$ and $|2\rangle$ on both 3LSs to be $2J$.

We solve the Schrödinger equation with an initial state of $|\psi_0\rangle = |200\rangle$, with the first 3LS in state $|2\rangle$ and the other two 3LSs in state $|0\rangle$. We calculate the probability of double excitations on the i th 3LS, which is given by

$$P_i^{(2)}(t) = \text{Tr}[\rho_S |2\rangle_{ii}\langle 2|], \quad (2)$$

where ρ_S is the density matrix of the system. We also use the negativity as a measure of the entanglement between the first and third 3LSs. This negativity, \mathcal{N}_{13} , is given by [23]

$$\mathcal{N}_{13} = \frac{\|\rho_{13}^{T_3}\|_1 - 1}{2}. \quad (3)$$

Here, $\rho_{13} = \text{Tr}_2[\rho_S]$ is the density matrix describing the first and third 3LSs after tracing out the second 3LS. Also, $\rho_{13}^{T_3}$ is the partial transpose of ρ_{13} with respect to the third 3LS and $\|\cdot\|_1$ is the trace norm. It is equivalently given by the absolute value of the sum of the negative eigenvalues of $\rho_{13}^{T_3}$ [23].

III. ANALYTIC SOLUTION

Since the initial state has a total of two excitations and the Hamiltonian conserves the total number of excitations, we write the Hamiltonian in matrix form in the two-excitation subspace. In the ordered basis $\{|200\rangle, |020\rangle, |002\rangle, |110\rangle, |101\rangle, |011\rangle\}$, the Hamiltonian in the two-excitation subspace is

$$H_2 = \begin{pmatrix} 2\omega & 0 & 0 & \sqrt{2}J & 0 & 0 \\ 0 & 2(\omega + \Delta) & 0 & \sqrt{2}J & 0 & \sqrt{2}J \\ 0 & 0 & 2\omega & 0 & 0 & \sqrt{2}J \\ \sqrt{2}J & \sqrt{2}J & 0 & 2\omega + \Delta & J & 0 \\ 0 & 0 & 0 & J & 2\omega & J \\ 0 & \sqrt{2}J & \sqrt{2}J & 0 & J & 2\omega + \Delta \end{pmatrix}. \quad (4)$$

If we define the angle θ such that

$$\tan \theta = \frac{2\sqrt{2}J}{\Delta} \tag{5}$$

and $0 < \theta < \pi$, then we can diagonalize the Hamiltonian H_2 to give the eigenvalues E_i ,

$$E_1 = 2\omega, \tag{6a}$$

$$E_2 = 2\omega + 2\sqrt{2}J \cot \theta, \tag{6b}$$

$$E_3 = 2\omega - 2\sqrt{2}J \tan \left(\frac{\theta}{2}\right), \tag{6c}$$

$$E_4 = 2\omega + 2\sqrt{2}J \cot \left(\frac{\theta}{2}\right), \tag{6d}$$

$$E_5 = 2\omega - \sqrt{2}J \tan \left(\frac{\theta}{2}\right), \tag{6e}$$

$$E_6 = 2\omega + \sqrt{2}J \cot \left(\frac{\theta}{2}\right), \tag{6f}$$

with corresponding eigenvectors $|\phi_i\rangle$,

$$|\phi_1\rangle = \frac{1}{2}(|200\rangle + |002\rangle - \sqrt{2}|101\rangle), \tag{7a}$$

$$|\phi_2\rangle = \frac{1}{2\sqrt{2}}(\sin \theta |200\rangle - 2 \sin \theta |020\rangle + \sin \theta |002\rangle + 2 \cos \theta |110\rangle + \sqrt{2} \sin \theta |101\rangle + 2 \cos \theta |011\rangle), \tag{7b}$$

$$|\phi_3\rangle = \frac{1}{2} \left[\cos^2 \left(\frac{\theta}{2}\right) |200\rangle + 2 \sin^2 \left(\frac{\theta}{2}\right) |020\rangle + \cos^2 \left(\frac{\theta}{2}\right) |002\rangle - \sin \theta |110\rangle + \sqrt{2} \cos^2 \left(\frac{\theta}{2}\right) |101\rangle - \sin \theta |011\rangle \right], \tag{7c}$$

$$|\phi_4\rangle = \frac{1}{2} \left[\sin^2 \left(\frac{\theta}{2}\right) |200\rangle + 2 \cos^2 \left(\frac{\theta}{2}\right) |020\rangle + \sin^2 \left(\frac{\theta}{2}\right) |002\rangle + \sin \theta |110\rangle + \sqrt{2} \sin^2 \left(\frac{\theta}{2}\right) |101\rangle + \sin \theta |011\rangle \right], \tag{7d}$$

$$|\phi_5\rangle = \frac{1}{\sqrt{2}} \left[\cos \left(\frac{\theta}{2}\right) |200\rangle - \cos \left(\frac{\theta}{2}\right) |002\rangle - \sin \left(\frac{\theta}{2}\right) |110\rangle + \sin \left(\frac{\theta}{2}\right) |011\rangle \right], \tag{7e}$$

$$|\phi_6\rangle = \frac{1}{\sqrt{2}} \left[\sin \left(\frac{\theta}{2}\right) |200\rangle - \sin \left(\frac{\theta}{2}\right) |002\rangle + \cos \left(\frac{\theta}{2}\right) |110\rangle - \cos \left(\frac{\theta}{2}\right) |011\rangle \right]. \tag{7f}$$

To simplify the expression for the wave function, we introduce

$$a_1(t) = \frac{1}{2} \left[e^{-i\sqrt{2} \cot \left(\frac{\theta}{2}\right) Jt} \sin^2 \left(\frac{\theta}{2}\right) + e^{i\sqrt{2} \tan \left(\frac{\theta}{2}\right) Jt} \cos^2 \left(\frac{\theta}{2}\right) + 1 \right], \tag{8a}$$

$$a_2(t) = \frac{1}{2\sqrt{2}} \left(e^{-i\sqrt{2} \cot \left(\frac{\theta}{2}\right) Jt} - e^{i\sqrt{2} \tan \left(\frac{\theta}{2}\right) Jt} \right) \sin \theta, \tag{8b}$$

$$a_3(t) = \frac{1}{2} \left[e^{-i\sqrt{2} \cot \left(\frac{\theta}{2}\right) Jt} \sin^2 \left(\frac{\theta}{2}\right) + e^{i\sqrt{2} \tan \left(\frac{\theta}{2}\right) Jt} \cos^2 \left(\frac{\theta}{2}\right) - 1 \right]. \tag{8c}$$

It can be shown that $|a_1|^2 + |a_2|^2 + |a_3|^2 = 1$. As derived in Appendix A, the wave function of the system at time t , $|\psi(t)\rangle$, starting from the initial state $|\psi_0\rangle$ is given by

$$|\psi(t)\rangle = a_1^2 |200\rangle + a_2^2 |020\rangle + a_3^2 |002\rangle + \sqrt{2} a_1 a_2 |110\rangle + \sqrt{2} a_1 a_3 |101\rangle + \sqrt{2} a_2 a_3 |011\rangle. \tag{9}$$

The double-excitation probability of the i th 3LS is given by

$$P_i^{(2)}(t) = |a_i|^4. \tag{10}$$

In terms of the detuning Δ , the double-excitation probabilities are given by

$$P_1^{(2)}(t) = \left[\cos^2 \left(\frac{\Delta - \sqrt{8J^2 + \Delta^2}}{4} t \right) - \frac{2J^2}{8J^2 + \Delta^2} \sin^2 \left(\frac{\sqrt{8J^2 + \Delta^2}}{2} t \right) + \frac{\Delta - \sqrt{8J^2 + \Delta^2}}{2\sqrt{8J^2 + \Delta^2}} \sin \left(\frac{\Delta}{2} t \right) \sin \left(\frac{\sqrt{8J^2 + \Delta^2}}{2} t \right) \right]^2, \tag{11a}$$

$$P_2^{(2)}(t) = \frac{16J^4}{(8J^2 + \Delta^2)^2} \sin^4 \left(\frac{1}{2} \sqrt{8J^2 + \Delta^2} t \right), \tag{11b}$$

$$P_3^{(2)}(t) = \left[\sin^2 \left(\frac{\Delta - \sqrt{8J^2 + \Delta^2}}{4} t \right) - \frac{2J^2}{8J^2 + \Delta^2} \sin^2 \left(\frac{\sqrt{8J^2 + \Delta^2}}{2} t \right) - \frac{\Delta - \sqrt{8J^2 + \Delta^2}}{2\sqrt{8J^2 + \Delta^2}} \sin \left(\frac{\Delta}{2} t \right) \sin \left(\frac{\sqrt{8J^2 + \Delta^2}}{2} t \right) \right]^2. \tag{11c}$$

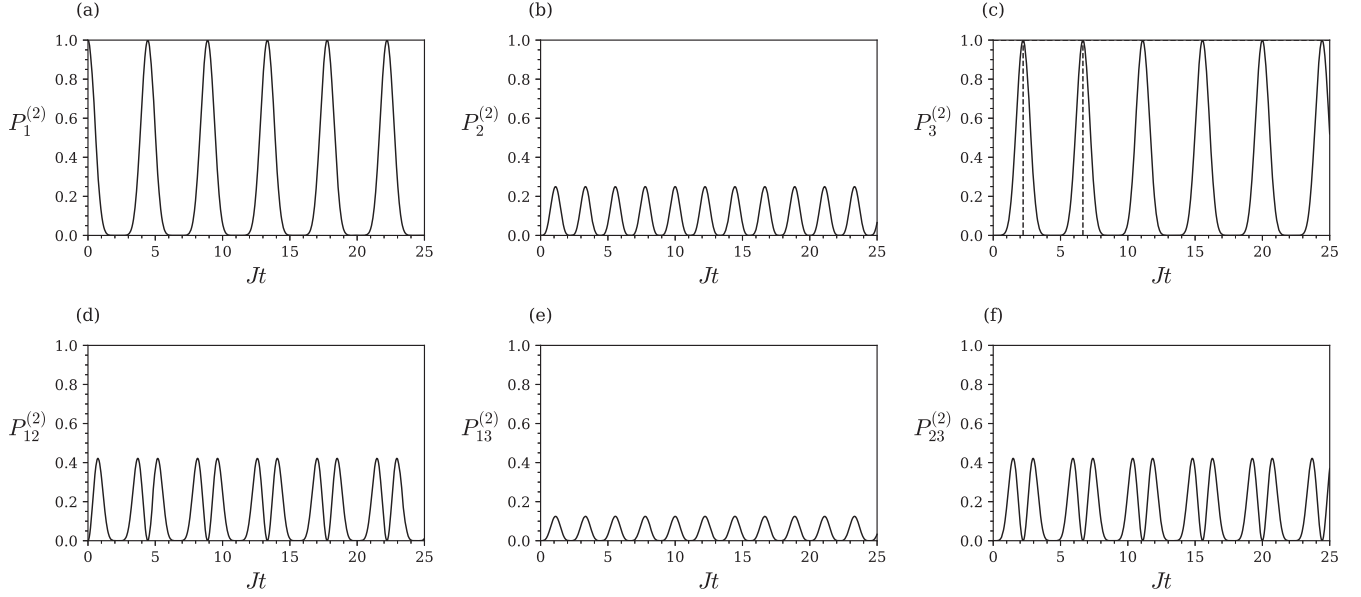


FIG. 2. Probabilities of the states (a) $|200\rangle$ ($P_1^{(2)}$), (b) $|020\rangle$ ($P_2^{(2)}$), (c) $|002\rangle$ ($P_3^{(2)}$), (d) $|110\rangle$ ($P_{12}^{(2)}$), (e) $|011\rangle$ ($P_{23}^{(2)}$), and (f) $|101\rangle$ ($P_{13}^{(2)}$) as functions of the dimensionless parameter Jt for $\Delta = 0$. The first two instances of perfect state transfer occur at $Jt = \frac{\pi}{\sqrt{2}}$ and $\frac{3\pi}{\sqrt{2}}$, as indicated by the dashed lines in (c).

From Eq. (8), $|a_i|^4$ is invariant under the transformation $\theta \rightarrow (\pi - \theta)$. This corresponds to the transformation $\Delta \rightarrow -\Delta$. Therefore, $P_i^{(2)}$ is invariant under a change in sign of Δ and only depends on the magnitude of Δ . In the special case of zero detuning, the probabilities are given by

$$P_1^{(2)}(t) = \cos^8\left(\frac{J}{\sqrt{2}}t\right), \quad (12a)$$

$$P_2^{(2)}(t) = \frac{1}{4} \sin^4(\sqrt{2}Jt), \quad (12b)$$

$$P_3^{(2)}(t) = \sin^8\left(\frac{J}{\sqrt{2}}t\right). \quad (12c)$$

The probability of a single excitation each on the i th and j th 3LSs is given by

$$P_{ij}^{(2)}(t) = 2|a_i a_j|^2. \quad (13)$$

Let us now define

$$p = |a_2|^8 + 10|a_2|^4|a_1 a_3|^2 + 7|a_1 a_3|^4, \quad (14a)$$

$$q = |a_2|^{12} + 15|a_2|^8|a_1 a_3|^2 + \frac{69}{2}|a_2|^4|a_1 a_3|^4 - 10|a_1 a_3|^6. \quad (14b)$$

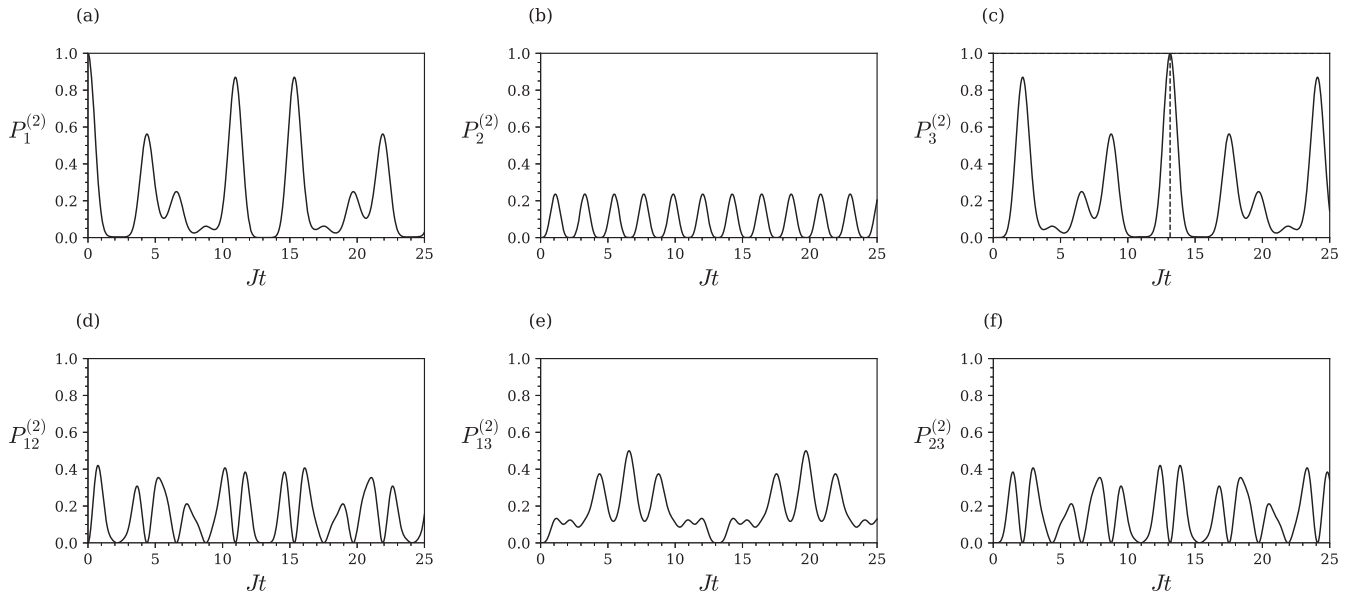


FIG. 3. Probabilities of the states (a) $|200\rangle$ ($P_1^{(2)}$), (b) $|020\rangle$ ($P_2^{(2)}$), (c) $|002\rangle$ ($P_3^{(2)}$), (d) $|110\rangle$ ($P_{12}^{(2)}$), (e) $|011\rangle$ ($P_{23}^{(2)}$), and (f) $|101\rangle$ ($P_{13}^{(2)}$) as functions of the dimensionless parameter Jt for $\Delta = \frac{2\sqrt{2}J}{\sqrt{35}}$. Perfect state transfer first occurs at $Jt = \frac{\pi}{\sqrt{2}}\sqrt{35}$, as indicated by the dashed line in (c).

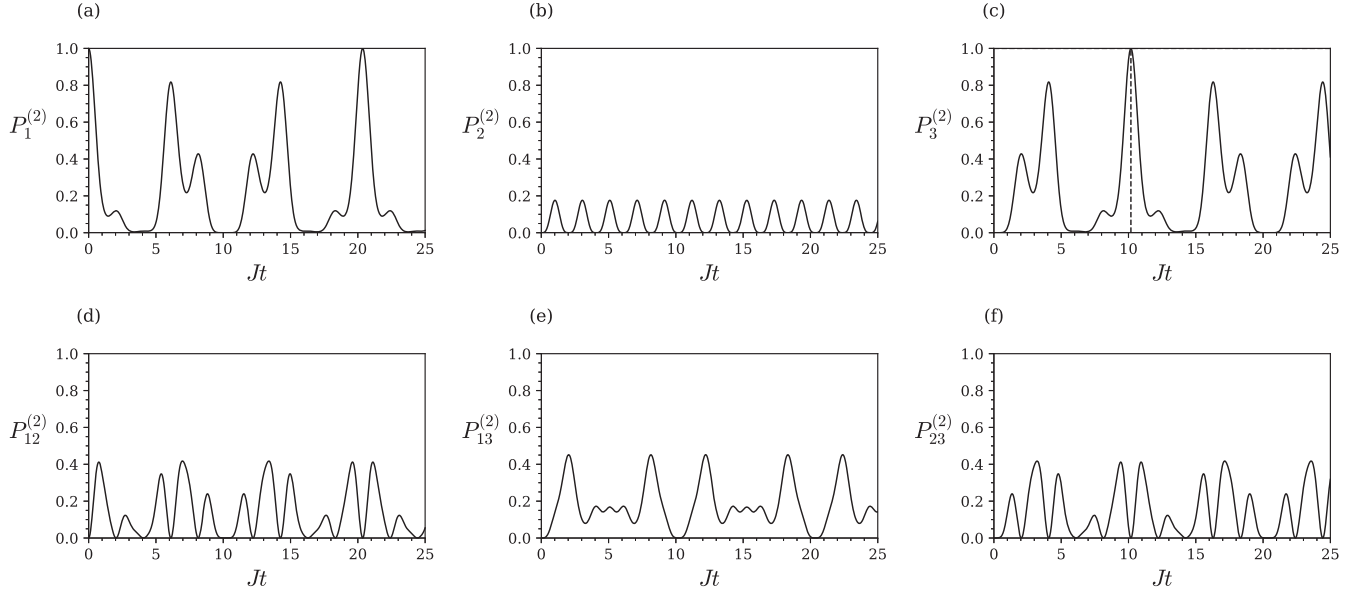


FIG. 4. Probabilities of the states (a) $|200\rangle$ ($P_1^{(2)}$), (b) $|020\rangle$ ($P_2^{(2)}$), (c) $|002\rangle$ ($P_3^{(2)}$), (d) $|110\rangle$ ($P_{12}^{(2)}$), (e) $|011\rangle$ ($P_{13}^{(2)}$), and (f) $|101\rangle$ ($P_{23}^{(2)}$) as functions of the dimensionless parameter Jt for $\Delta = \frac{4\sqrt{2}J}{\sqrt{21}}$. Perfect state transfer first occurs at $Jt = \frac{\pi}{\sqrt{2}}\sqrt{21}$, as indicated by the dashed line in (c).

As derived in Appendix B, the negativity is then given by

$$\begin{aligned} \mathcal{N}_{13}(t) = & (|a_1|^2 + |a_3|^2)(\sqrt{|a_2|^4 + 2|a_1a_3|^2} - |a_2|^2) \\ & + \frac{2}{3}\sqrt{p} \sin \left[\frac{1}{3} \arccos \left(\frac{q}{p\sqrt{p}} \right) + \frac{\pi}{6} \right] \\ & - \frac{1}{3}(|a_2|^4 + 2|a_1a_3|^2). \end{aligned} \quad (15)$$

IV. PERFECT STATE TRANSFER AND MAXIMAL ENTANGLEMENT

As derived in Appendix C, we get periodic perfect state transfer of the double excitation to the third 3LS for angles θ_p that satisfy

$$\cot^2 \left(\frac{\theta_p}{2} \right) = \frac{2n+1}{2m+1}, \quad (16)$$

where $n, m = 0, 1, 2, \dots$. This corresponds to detunings of

$$\Delta_p = \frac{2\sqrt{2}J(n-m)}{\sqrt{(2n+1)(2m+1)}}. \quad (17)$$

A positive detuning is obtained when $n > m$ and a negative detuning of equal magnitude is obtained by interchanging n and m . Perfect state transfer occurs at time τ_p , given by

$$\tau_p = \frac{\pi\sqrt{(2n+1)(2m+1)}}{\sqrt{2}J}. \quad (18)$$

Equation (18) gives the first occurrence of perfect state transfer for values of n and m , which result in a fraction for the right-hand side of Eq. (16) that is irreducible. For example, for $n = 2$ and $m = 7$, the right-hand side of Eq. (16) is $\frac{5}{15}$ and we get $\tau_p = \frac{5\pi}{J}\sqrt{\frac{3}{2}}$. However, the time for the first occurrence of perfect state transfer would be obtained by reducing $\frac{5}{15}$ to $\frac{1}{3}$, which corresponds to $n = 0$ and $m = 1$, resulting in $\tau_p = \frac{\pi}{J}\sqrt{\frac{3}{2}}$.

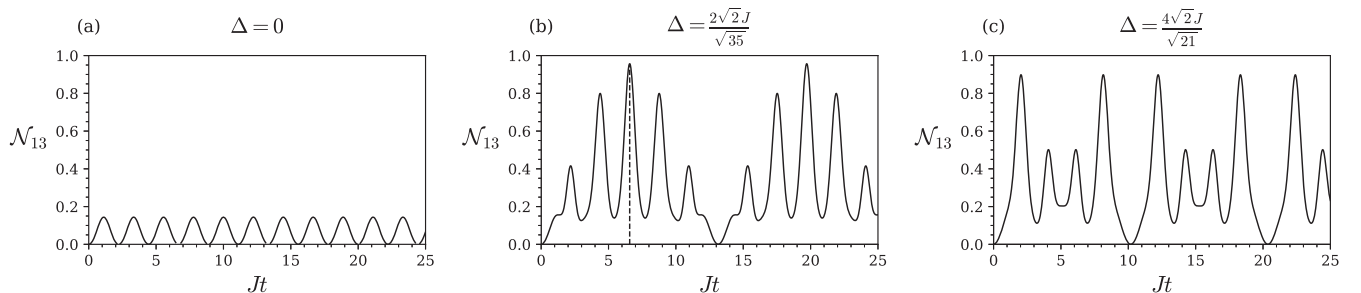


FIG. 5. The negativity \mathcal{N}_{13} as a function of the dimensionless time Jt for (a) $\Delta = 0$, (b) $\Delta = \frac{2\sqrt{2}J}{\sqrt{35}}$, and (c) $\Delta = \frac{4\sqrt{2}J}{\sqrt{21}}$. Maximal entanglement first occurs at $Jt = \frac{\pi}{2}\sqrt{35}$ for $\Delta = \frac{2\sqrt{2}J}{\sqrt{35}}$, as indicated by the dashed line in (b).

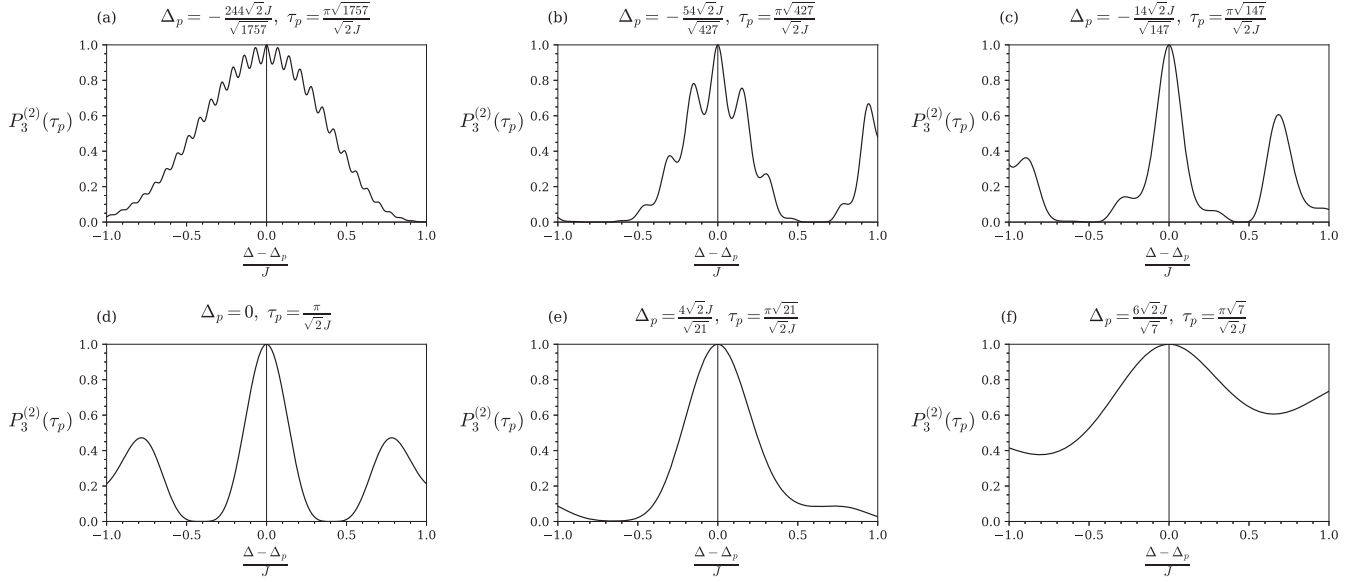


FIG. 6. Double-excitation probability $P_3^{(2)}$ of the third 3LS as a function of Δ at time τ_p for six values of Δ_p and τ_p .

As derived in Appendix D, the maximum value that the negativity reaches in the evolution of the system is $\mathcal{N}_{\max} = \frac{1}{4} + \frac{1}{\sqrt{2}} \approx 0.9571$. This occurs for detunings that satisfy Eq. (17), with the added constraint that $(n - m)$ is odd. Therefore, maximal entanglement can only be obtained when there is perfect state transfer. The maximal entanglement occurs at time τ_N given by $\tau_N = \frac{1}{2}\tau_p$. The wave function at time τ_N is given by

$$|\psi(\tau_N)\rangle = \frac{i}{2}|200\rangle + \frac{(-1)^n}{\sqrt{2}}|101\rangle - \frac{i}{2}|002\rangle. \quad (19)$$

V. RESULTS

A. Perfect state transfer

We first consider three detunings, $\Delta = 0, \frac{2\sqrt{2}J}{\sqrt{35}}, \frac{4\sqrt{2}J}{\sqrt{21}}$, that give perfect state transfer. Figure 2 shows the results for the probabilities $P_1^{(2)}$ (for state $|200\rangle$), $P_2^{(2)}$ (for state $|020\rangle$), $P_3^{(2)}$ (for state $|002\rangle$), $P_{12}^{(2)}$ (for state $|110\rangle$), $P_{13}^{(2)}$ (for state $|101\rangle$), and $P_{23}^{(2)}$ (for state $|011\rangle$) as functions of the dimensionless parameter Jt for $\Delta = 0$. The $\Delta = 0$ case satisfies Eq. (17) and the first instance of perfect state transfer occurs at $Jt = \frac{\pi}{\sqrt{2}}$, with an interval of $Jt = \sqrt{2}\pi$ between consecutive occurrences. The double-excitation probabilities $P_1^{(2)}$ and $P_3^{(2)}$ exhibit oscillations between 0 and 1 with an angular frequency of $\sqrt{2}J$. On the other hand, $P_2^{(2)}$ oscillates between 0 and 0.25 with an angular frequency of $2\sqrt{2}J$.

Figure 3 shows the results for the various probabilities for $\Delta = \frac{2\sqrt{2}J}{\sqrt{35}}$. This value of Δ satisfies the perfect state transfer condition in Eq. (17) for $n = 3$ and $m = 2$. The first instance of perfect state transfer occurs at $Jt = \frac{\pi}{\sqrt{2}}\sqrt{35}$. The double-excitation probabilities $P_1^{(2)}$ and $P_3^{(2)}$ exhibit oscillations between 0 and 1, while $P_2^{(2)}$ oscillates

between 0 and 0.236, with an angular frequency of $2.87J$.

Figure 4 shows the results for the various probabilities for $\Delta = \frac{4\sqrt{2}J}{\sqrt{21}}$. This value of Δ satisfies the perfect state transfer condition in Eq. (17) for $n = 3$ and $m = 1$. The first instance of perfect state transfer occurs at $Jt = \frac{\pi}{\sqrt{2}}\sqrt{21}$. The double-excitation probabilities $P_1^{(2)}$ and $P_3^{(2)}$ exhibit oscillations between 0 and 1, while $P_2^{(2)}$ oscillates between 0 and 0.176 with an angular frequency of $3.09J$.

For all three detunings, the probabilities $P_{12}^{(2)}$, $P_{13}^{(2)}$, and $P_{23}^{(2)}$ exhibit oscillations, indicating the propagation of single excitations in the system in superposition with the double excitations.

Figure 5 shows the results for the negativity \mathcal{N}_{13} for the detunings $\Delta = 0, \frac{2\sqrt{2}J}{\sqrt{35}}, \frac{4\sqrt{2}J}{\sqrt{21}}$ as functions of the dimensionless parameter Jt . Figure 5(a) shows that for $\Delta = 0$, the negativity oscillates between 0 and 0.144 with an angular frequency of $2\sqrt{2}J$. Even though we have perfect state transfer in this case, maximal entanglement is not achieved since $n - m = 0$, which is not odd. Figure 5(b) shows that for $\Delta = \frac{2\sqrt{2}J}{\sqrt{35}}$, the negativity oscillates between 0 and 0.9571. Since in this case $n - m = 1$, which is odd, maximal entanglement is obtained. The first occurrence of maximal entanglement is at $Jt = \frac{\pi}{2\sqrt{2}}\sqrt{35}$. Figure 5(c) shows that for $\Delta = \frac{4\sqrt{2}J}{\sqrt{21}}$, the negativity oscillates between 0 and 0.899. In this case, $n - m = 2$, which is not odd, so maximal entanglement is not achieved.

TABLE I. Detuning values and associated times for perfect state transfer.

Δ_p	$-\frac{244\sqrt{2}J}{\sqrt{1757}}$	$-\frac{54\sqrt{2}J}{\sqrt{427}}$	$-\frac{14\sqrt{2}J}{\sqrt{147}}$	0	$\frac{4\sqrt{2}J}{\sqrt{21}}$	$\frac{6\sqrt{2}J}{\sqrt{7}}$
τ_p	$\frac{\pi\sqrt{1757}}{\sqrt{2}J}$	$\frac{\pi\sqrt{427}}{\sqrt{2}J}$	$\frac{\pi\sqrt{147}}{\sqrt{2}J}$	$\frac{\pi}{\sqrt{2}J}$	$\frac{\pi\sqrt{21}}{\sqrt{2}J}$	$\frac{\pi\sqrt{7}}{\sqrt{2}J}$

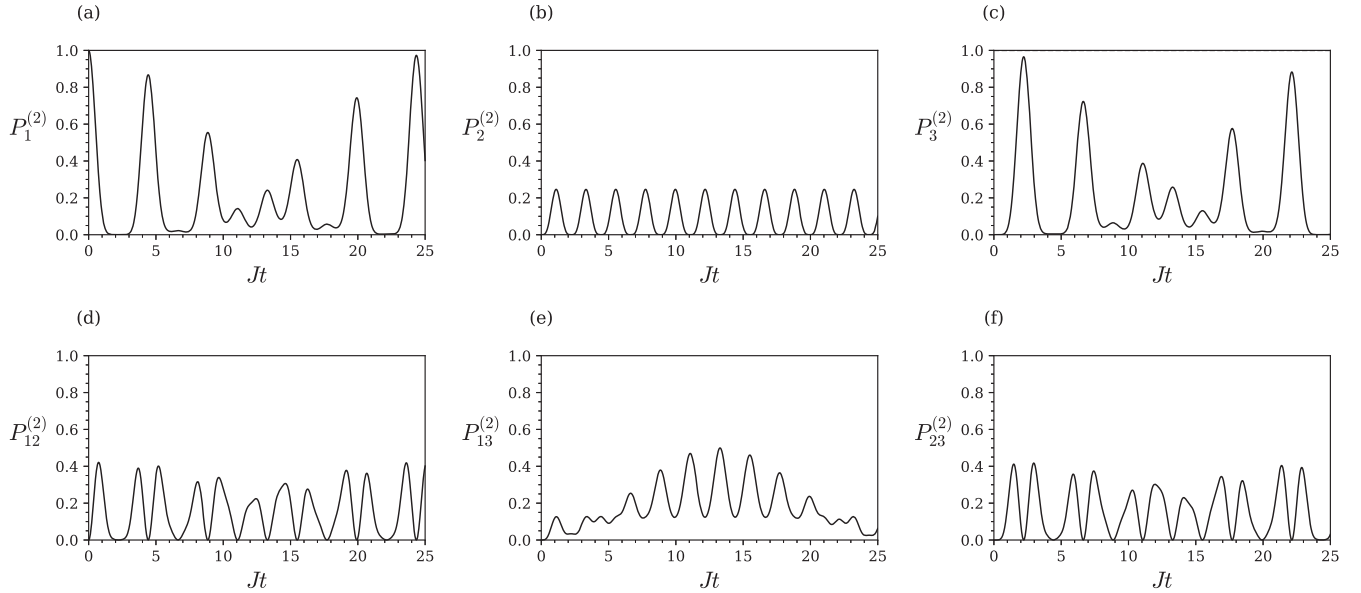


FIG. 7. Probabilities of the states (a) $|200\rangle$ ($P_1^{(2)}$), (b) $|020\rangle$ ($P_2^{(2)}$), (c) $|002\rangle$ ($P_3^{(2)}$), (d) $|110\rangle$ ($P_{12}^{(2)}$), (e) $|011\rangle$ ($P_{13}^{(2)}$), and (f) $|101\rangle$ ($P_{23}^{(2)}$) as functions of the dimensionless parameter Jt for $\Delta = \frac{\sqrt{2}}{\sqrt{35}}$.

Figure 6 shows how the double-excitation probability of the third 3LS varies with the detuning for the six occurrences of perfect state transfer given in Table I. Aside from the case of $\Delta = 0$, there is a general trend where the width of the resonance peak increases as the magnitude of the detuning increases.

B. Imperfect state transfer

We now consider two detunings, $\Delta = \frac{\sqrt{2}J}{\sqrt{35}}$, J , that do not satisfy Eq. (17) and, therefore, do not give perfect state transfer. Figure 7 shows the results for the various probabilities

for $\Delta = \frac{\sqrt{2}J}{\sqrt{35}}$. The double-excitation probabilities $P_1^{(2)}$ and $P_3^{(2)}$ show oscillations with an angular frequency of $2.84J$ with varying peak amplitudes. The maximum value of $P_3^{(2)}$ over the plotted interval is 0.966 and we get near-perfect state transfer. The double-excitation probability $P_2^{(2)}$ oscillates between 0 and 0.246, also with an angular frequency of $2.84J$.

Figure 8 shows the results for the various probabilities for $\Delta = J$. The double-excitation probability $P_1^{(2)}$ oscillates between 0.012 and 1 with an angular frequency of J , while the double-excitation probability $P_3^{(2)}$ oscillates between 0 and

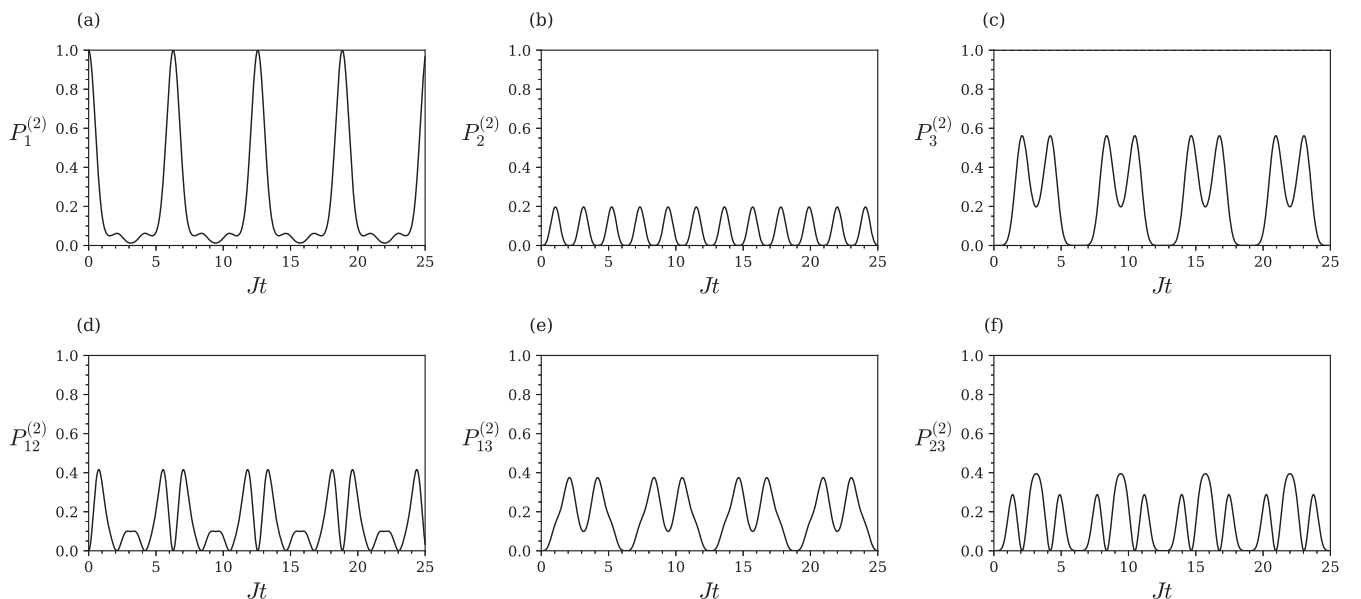


FIG. 8. Probabilities of the states (a) $|200\rangle$ ($P_1^{(2)}$), (b) $|020\rangle$ ($P_2^{(2)}$), (c) $|002\rangle$ ($P_3^{(2)}$), (d) $|110\rangle$ ($P_{12}^{(2)}$), (e) $|011\rangle$ ($P_{13}^{(2)}$), and (f) $|101\rangle$ ($P_{23}^{(2)}$) as functions of the dimensionless parameter Jt for $\Delta = J$.

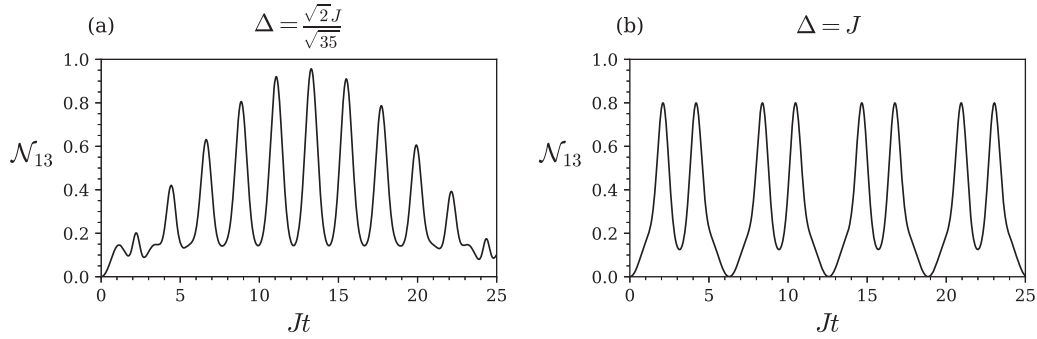


FIG. 9. The negativity \mathcal{N}_{13} as a function of the dimensionless parameter Jt for (a) $\Delta = \frac{\sqrt{2}J}{\sqrt{35}}$ and (b) $\Delta = J$.

0.562 with the same frequency as $P_1^{(2)}$ but exhibiting two maxima and two minima within each cycle. Also, $P_2^{(2)}$ oscillates between 0 and 0.198 with an angular frequency of $3J$.

Figure 9 shows the results for the negativity \mathcal{N}_{13} for the detunings $\Delta = \frac{\sqrt{2}J}{\sqrt{35}}, J$ as functions of the dimensionless parameter Jt . Figure 9(a) shows that for $\Delta = \frac{\sqrt{2}J}{\sqrt{35}}$, \mathcal{N}_{13} oscillates with angular frequency $2.84J$. Within the plotted interval, \mathcal{N}_{13} has a maximum value of 0.9569. In this case, where we have near-perfect state transfer, we also get near-maximal entanglement. Figure 9(b) shows that for $\Delta = J$, the negativity oscillates between 0 and 0.800 with angular frequency J and exhibits two maxima and two minima within each cycle.

Figure 10 shows how the double-excitation probability of the third 3LS varies with the detuning at the time of maximum probability for near-perfect state transfer with detuning $\Delta_I = \frac{\sqrt{2}J}{\sqrt{35}}$. At that time, there is a perfect state transfer at a detuning less than Δ_I and the double-excitation probability slowly decays away from that maximum.

VI. CONCLUSION

We analytically determined the detuning condition, as given by Eq. (17), for perfect state transfer of a double

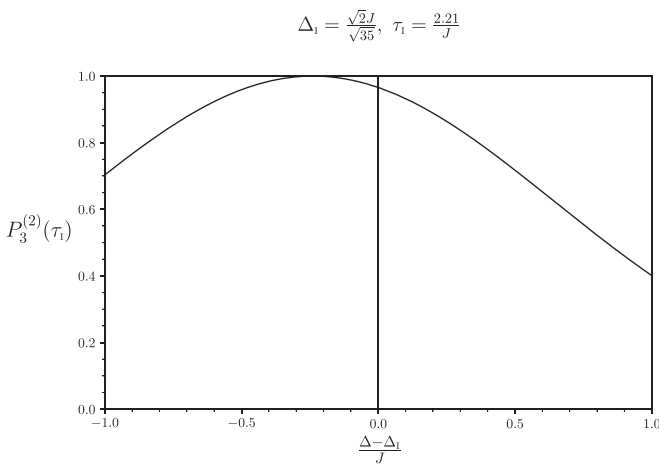


FIG. 10. Double-excitation probability $P_3^{(2)}$ of the third 3LS as a function of Δ at the time of maximum probability $\tau_1 = \frac{2.21}{J}$ for the detuning $\Delta_I = \frac{\sqrt{2}J}{\sqrt{35}}$.

excitation in a trimer of 3LSs with a detuning on the central 3LS. We also determined the times at which perfect state transfer occurred. Additionally, we determined that maximal entanglement between the first and third 3LSs only occurred for nonzero detunings that gave perfect state transfer, with the constraint that $(n - m)$ from Eq. (17) was odd. We found that maximal entanglement preceded perfect state transfer with an occurrence time that was half the time at which perfect state transfer occurred. We also found that values for the detuning that do not satisfy the perfect state transfer condition can also give near-perfect state transfer as well as near-maximal entanglement. These results are important as we have analytically shown conditions for perfect state transfer of double excitations that can be engineered using only the detuning of a central 3LS in the model. We have also demonstrated how to achieve maximal entanglement between distant 3LSs without the need for any dynamical control.

Since the perfect state transfer and maximal entanglement are periodic, it is possible to perform information processing on the transmitted qutrits along an array of trimers acting as a quantum bus in a sequential and controllable manner. Also, we can evolve multiple systems at the same time and select the measurement times based on the length of time needed for processing in different paths. These results should have applications in quantum information processing and quantum communication. Specific applications could be, for instance, in quantum repeaters, quantum memories, quantum key distribution, and quantum error correction.

Since we have accurate time intervals in the probabilities, the time difference between two clocks, each positioned at the end of a chain, can be calibrated. Therefore, applications in clock synchronization are possible. Additionally, the periodic occurrence of maximal entanglement allows for the preparation of entangled qutrits that could be used in entanglement swapping, which has applications in quantum teleportation. However, because the perfect state transfer and maximal entanglement are periodic, measurements would have to be done within a small time frame since the time for which the state exists at the end of the trimer is very short compared to the repetition time. This could prove challenging for quantum measurements on the state. If a longer time is needed for measurement, then a technique such as a dynamical decoupling can be used since the state exists for a longer period of time in that case.

APPENDIX A: DERIVATION OF THE WAVE FUNCTION

The solution of the time-independent Schrödinger equation for the Hamiltonian in Eq. (1) with initial state $|\psi_0\rangle$ results in the wave function

$$|\psi(t)\rangle = e^{-iHt}|\psi_0\rangle. \quad (\text{A1})$$

Expanding the matrix exponential using the eigenvalues and eigenvectors in Eqs. (6) and (7) gives

$$\begin{aligned} |\psi(t)\rangle &= \left(\sum_{i=1}^6 e^{-iE_i t} |\phi_i\rangle \langle \phi_i| \right) |\psi_0\rangle \\ &= \sum_{i=1}^6 e^{-iE_i t} \langle \phi_i | 200 \rangle |\phi_i\rangle. \end{aligned} \quad (\text{A2})$$

If we let $\alpha = e^{i\sqrt{2}\tan(\frac{\theta}{2})t}$ and $\beta = e^{-i\sqrt{2}\cot(\frac{\theta}{2})t}$, then the wave function becomes

$$\begin{aligned} |\psi(t)\rangle &= e^{-i2\omega t} \left[\frac{1}{2} |\phi_1\rangle + \frac{1}{2\sqrt{2}} \alpha \beta \sin \theta |\phi_2\rangle + \frac{1}{2} \alpha^2 \cos^2 \left(\frac{\theta}{2} \right) |\phi_3\rangle \right. \\ &\quad \left. + \frac{1}{2} \beta^2 \sin^2 \left(\frac{\theta}{2} \right) |\phi_4\rangle + \frac{1}{\sqrt{2}} \alpha \cos \left(\frac{\theta}{2} \right) |\phi_5\rangle + \frac{1}{\sqrt{2}} \beta \sin \left(\frac{\theta}{2} \right) |\phi_6\rangle \right]. \end{aligned} \quad (\text{A3})$$

Dropping the global phase $e^{-i2\omega t}$ and substituting for the eigenvectors using Eq. (7) gives

$$\begin{aligned} |\psi(t)\rangle &= \left[\frac{1}{4} + \frac{1}{8} \alpha \beta \sin^2 \theta + \frac{1}{4} \alpha^2 \cos^4 \left(\frac{\theta}{2} \right) + \frac{1}{4} \beta^2 \sin^4 \left(\frac{\theta}{2} \right) + \frac{1}{2} \alpha \cos^2 \left(\frac{\theta}{2} \right) + \frac{1}{2} \beta \sin^2 \left(\frac{\theta}{2} \right) \right] |200\rangle \\ &\quad + \left(-\frac{1}{4} \alpha \beta \sin^2 \theta + \frac{1}{8} \alpha^2 \sin^2 \theta + \frac{1}{8} \beta^2 \sin^2 \theta \right) |020\rangle \\ &\quad + \left[\frac{1}{4} + \frac{1}{8} \alpha \beta \sin^2 \theta + \frac{1}{4} \alpha^2 \cos^4 \left(\frac{\theta}{2} \right) + \frac{1}{4} \beta^2 \sin^4 \left(\frac{\theta}{2} \right) - \frac{1}{2} \alpha \cos^2 \left(\frac{\theta}{2} \right) - \frac{1}{2} \beta \sin^2 \left(\frac{\theta}{2} \right) \right] |002\rangle \\ &\quad + \left[\frac{1}{4} \alpha \beta \sin \theta \cos \theta - \frac{1}{4} \alpha^2 \sin \theta \cos^2 \left(\frac{\theta}{2} \right) + \frac{1}{4} \beta^2 \sin \theta \sin^2 \left(\frac{\theta}{2} \right) \right. \\ &\quad \left. - \frac{1}{2} \alpha \sin \left(\frac{\theta}{2} \right) \cos \left(\frac{\theta}{2} \right) + \frac{1}{2} \beta \sin \left(\frac{\theta}{2} \right) \cos \left(\frac{\theta}{2} \right) \right] |110\rangle \\ &\quad + \left[-\frac{1}{2\sqrt{2}} + \frac{1}{4\sqrt{2}} \alpha \beta \sin^2 \theta + \frac{1}{2\sqrt{2}} \alpha^2 \cos^4 \left(\frac{\theta}{2} \right) + \frac{1}{2\sqrt{2}} \beta^2 \sin^4 \left(\frac{\theta}{2} \right) \right] |101\rangle \\ &\quad + \left[\frac{1}{4} \alpha \beta \sin \theta \cos \theta - \frac{1}{4} \alpha^2 \sin \theta \cos^2 \left(\frac{\theta}{2} \right) + \frac{1}{4} \beta^2 \sin \theta \sin^2 \left(\frac{\theta}{2} \right) \right. \\ &\quad \left. + \frac{1}{2} \alpha \sin \left(\frac{\theta}{2} \right) \cos \left(\frac{\theta}{2} \right) - \frac{1}{2} \beta \sin \left(\frac{\theta}{2} \right) \cos \left(\frac{\theta}{2} \right) \right] |011\rangle. \end{aligned} \quad (\text{A4})$$

By using trigonometric identities and simplifying, this becomes

$$\begin{aligned} |\psi(t)\rangle &= \frac{1}{4} \left[\beta \sin^2 \left(\frac{\theta}{2} \right) + \alpha \cos^2 \left(\frac{\theta}{2} \right) + 1 \right]^2 |200\rangle + \frac{1}{8} (\beta - \alpha)^2 \sin^2 \theta |020\rangle \\ &\quad + \frac{1}{4} \left[\beta \sin^2 \left(\frac{\theta}{2} \right) + \alpha \cos^2 \left(\frac{\theta}{2} \right) - 1 \right]^2 |002\rangle + \frac{1}{4} \left[\beta \sin^2 \left(\frac{\theta}{2} \right) + \alpha \cos^2 \left(\frac{\theta}{2} \right) + 1 \right] (\beta - \alpha) \sin \theta |110\rangle \\ &\quad + \frac{1}{2\sqrt{2}} \left[\beta \sin^2 \left(\frac{\theta}{2} \right) + \alpha \cos^2 \left(\frac{\theta}{2} \right) + 1 \right] \left[\beta \sin^2 \left(\frac{\theta}{2} \right) + \alpha \cos^2 \left(\frac{\theta}{2} \right) - 1 \right] |101\rangle \\ &\quad + \frac{1}{4} \left[\beta \sin^2 \left(\frac{\theta}{2} \right) + \alpha \cos^2 \left(\frac{\theta}{2} \right) - 1 \right] (\beta - \alpha) \sin \theta |011\rangle \\ &= a_1^2 |200\rangle + a_2^2 |020\rangle + a_3^2 |002\rangle + \sqrt{2} a_1 a_2 |110\rangle + \sqrt{2} a_1 a_3 |101\rangle + \sqrt{2} a_2 a_3 |011\rangle, \end{aligned} \quad (\text{A5})$$

where a_1 , a_2 , and a_3 are defined as given in Eq. (8), giving the result for the wave function shown in Eq. (9).

APPENDIX B: DERIVATION OF THE NEGATIVITY

The density matrix of the system is given by

$$\rho_S = |\psi(t)\rangle\langle\psi(t)|. \quad (\text{B1})$$

The reduced density matrix describing the first and third 3LSs is then given by

$$\rho_{13} = \text{Tr}_2[\rho_S] = \sum_{j=0}^2 {}_2\langle j|\rho_S|j\rangle_2 = \sum_{j=0}^2 {}_2\langle j|\psi(t)\rangle\langle\psi(t)|j\rangle_2. \quad (\text{B2})$$

Let

$$\begin{aligned} |\Psi_0\rangle &= {}_2\langle 0|\psi(t)\rangle \\ &= {}_2\langle 0|(a_1^2|200\rangle + a_2^2|020\rangle + a_3^2|002\rangle + \sqrt{2}a_1a_2|110\rangle + \sqrt{2}a_1a_3|101\rangle + \sqrt{2}a_2a_3|011\rangle) \\ &= a_1^2|20\rangle + a_3^2|02\rangle + \sqrt{2}a_1a_3|11\rangle, \end{aligned} \quad (\text{B3a})$$

$$\begin{aligned} |\Psi_1\rangle &= {}_2\langle 1|\psi(t)\rangle \\ &= {}_2\langle 1|(a_1^2|200\rangle + a_2^2|020\rangle + a_3^2|002\rangle + \sqrt{2}a_1a_2|110\rangle + \sqrt{2}a_1a_3|101\rangle + \sqrt{2}a_2a_3|011\rangle) \\ &= \sqrt{2}a_1a_2|10\rangle + \sqrt{2}a_2a_3|01\rangle, \end{aligned} \quad (\text{B3b})$$

$$\begin{aligned} |\Psi_2\rangle &= {}_2\langle 2|\psi(t)\rangle \\ &= {}_2\langle 2|(a_1^2|200\rangle + a_2^2|020\rangle + a_3^2|002\rangle + \sqrt{2}a_1a_2|110\rangle + \sqrt{2}a_1a_3|101\rangle + \sqrt{2}a_2a_3|011\rangle) \\ &= a_2^2|00\rangle. \end{aligned} \quad (\text{B3c})$$

Then we can write

$$\rho_{13} = \sum_{j=0}^2 |\Psi_j\rangle\langle\Psi_j|. \quad (\text{B4})$$

We can write the partial transpose of ρ_{13} with respect to the third 3LS in the ordered basis $\{|00\rangle, |10\rangle, |01\rangle, |20\rangle, |11\rangle, |02\rangle, |21\rangle, |12\rangle, |22\rangle\}$ as

$$\rho_{13}^{\mathcal{T}_3} = \begin{pmatrix} |a_2|^4 & 0 & 0 & 0 & 2a_1^*a_3|a_2|^2 & 0 & 0 & 0 & (a_1^*a_3)^2 \\ 0 & 2|a_1a_2|^2 & 0 & 0 & 0 & 0 & \sqrt{2}a_1^*a_3|a_1|^2 & 0 & 0 \\ 0 & 0 & 2|a_2a_3|^2 & 0 & 0 & 0 & 0 & \sqrt{2}a_1^*a_3|a_3|^2 & 0 \\ 0 & 0 & 0 & |a_1|^4 & 0 & 0 & 0 & 0 & 0 \\ 2a_1a_3^*|a_2|^2 & 0 & 0 & 0 & 2|a_1a_3|^2 & 0 & 0 & 0 & 0 \\ 0 & 0 & 0 & 0 & 0 & |a_3|^4 & 0 & 0 & 0 \\ 0 & \sqrt{2}a_1a_3^*|a_1|^2 & 0 & 0 & 0 & 0 & 0 & 0 & 0 \\ 0 & 0 & \sqrt{2}a_1a_3^*|a_3|^2 & 0 & 0 & 0 & 0 & 0 & 0 \\ (a_1a_3^*)^2 & 0 & 0 & 0 & 0 & 0 & 0 & 0 & 0 \end{pmatrix}. \quad (\text{B5})$$

The first six eigenvalues of this matrix are given by

$$\lambda_1 = |a_1|^4, \quad (\text{B6a})$$

$$\lambda_2 = |a_3|^4, \quad (\text{B6b})$$

$$\lambda_3 = |a_1|^2 \left(|a_2|^2 - \sqrt{|a_2|^4 + 2|a_1a_3|^2} \right), \quad (\text{B6c})$$

$$\lambda_4 = |a_1|^2 \left(|a_2|^2 + \sqrt{|a_2|^4 + 2|a_1a_3|^2} \right), \quad (\text{B6d})$$

$$\lambda_5 = |a_3|^2 \left(|a_2|^2 - \sqrt{|a_2|^4 + 2|a_1a_3|^2} \right), \quad (\text{B6e})$$

$$\lambda_6 = |a_3|^2 \left(|a_2|^2 + \sqrt{|a_2|^4 + 2|a_1a_3|^2} \right). \quad (\text{B6f})$$

The remaining three eigenvalues, λ_7 , λ_8 , and λ_9 are the roots of the cubic equation

$$x^3 - (|a_2|^4 + 2|a_1a_3|^2)x^2 - |a_1a_3|^2(|a_1a_3|^2 + 2|a_2|^4)x + 2|a_1a_3|^6 = 0. \tag{B7}$$

If we define p and q as given in Eq. (14), then the roots of the cubic equation in trigonometric form are given in increasing order by

$$\lambda_7 = -\frac{2}{3}\sqrt{p} \sin \left[\frac{1}{3} \arccos \left(\frac{q}{p\sqrt{p}} \right) + \frac{\pi}{6} \right] + \frac{1}{3}(|a_2|^4 + 2|a_1a_3|^2), \tag{B8a}$$

$$\lambda_8 = -\frac{2}{3}\sqrt{p} \sin \left[\frac{1}{3} \arccos \left(\frac{q}{p\sqrt{p}} \right) + \frac{5\pi}{6} \right] + \frac{1}{3}(|a_2|^4 + 2|a_1a_3|^2), \tag{B8b}$$

$$\lambda_9 = -\frac{2}{3}\sqrt{p} \sin \left[\frac{1}{3} \arccos \left(\frac{q}{p\sqrt{p}} \right) + \frac{3\pi}{2} \right] + \frac{1}{3}(|a_2|^4 + 2|a_1a_3|^2). \tag{B8c}$$

From the properties of the roots of the cubic equation, we have

$$\lambda_7\lambda_8\lambda_9 = -2|a_1a_3|^6 \leq 0 \quad \text{and} \quad \lambda_7 + \lambda_8 + \lambda_9 = |a_2|^4 + 2|a_1a_3|^2 \geq 0. \tag{B9}$$

Therefore, at most, one of the roots is negative and if none of them are negative then at least one of them must be zero. Thus, the eigenvalues that are either zero or negative are λ_3 , λ_5 , and λ_7 . Since adding a zero eigenvalue has no effect on the sum, the negativity is given by

$$\begin{aligned} \mathcal{N}_{13}(t) &= |\lambda_3 + \lambda_5 + \lambda_7| \\ &= -\lambda_3 - \lambda_5 - \lambda_7 \\ &= (|a_1|^2 + |a_3|^2) \left(\sqrt{|a_2|^4 + 2|a_1a_3|^2} - |a_2|^2 \right) + \frac{2}{3}\sqrt{p} \sin \left[\frac{1}{3} \arccos \left(\frac{q}{p\sqrt{p}} \right) + \frac{\pi}{6} \right] - \frac{1}{3}(|a_2|^4 + 2|a_1a_3|^2), \end{aligned} \tag{B10}$$

giving the result in Eq. (15).

APPENDIX C: DERIVATION OF THE PERFECT STATE TRANSFER CRITERION

From the triangle inequality for the complex numbers z_1 , z_2 , and z_3 , we have

$$|z_1 + z_2 + z_3| \leq |z_1| + |z_2| + |z_3|, \tag{C1}$$

with equality when

$$\arg(z_1) \equiv \arg(z_2) \equiv \arg(z_3) \pmod{2\pi}. \tag{C2}$$

Therefore,

$$\begin{aligned} P_3^{(2)}(t) &= |a_3|^4 \\ &= \left| \frac{1}{2} \left[e^{-i\sqrt{2}\cot(\frac{\theta}{2})Jt} \sin^2 \left(\frac{\theta}{2} \right) + e^{i\sqrt{2}\tan(\frac{\theta}{2})Jt} \cos^2 \left(\frac{\theta}{2} \right) - 1 \right] \right|^4 \\ &= \frac{1}{16} \left| e^{-i\sqrt{2}\cot(\frac{\theta}{2})Jt} \sin^2 \left(\frac{\theta}{2} \right) + e^{i\sqrt{2}\tan(\frac{\theta}{2})Jt} \cos^2 \left(\frac{\theta}{2} \right) - 1 \right|^4 \\ &\leq \frac{1}{16} \left[\left| e^{-i\sqrt{2}\cot(\frac{\theta}{2})Jt} \sin^2 \left(\frac{\theta}{2} \right) \right| + \left| e^{i\sqrt{2}\tan(\frac{\theta}{2})Jt} \cos^2 \left(\frac{\theta}{2} \right) \right| + |-1| \right]^4 \\ &= \frac{1}{16} \left[\left| \sin^2 \left(\frac{\theta}{2} \right) \right| + \left| \cos^2 \left(\frac{\theta}{2} \right) \right| + 1 \right]^4 \\ &= \frac{1}{16} \left[\sin^2 \left(\frac{\theta}{2} \right) + \cos^2 \left(\frac{\theta}{2} \right) + 1 \right]^4 \\ &= \frac{1}{16} (2)^4 \\ &= 1, \end{aligned} \tag{C3}$$

with equality when

$$\arg \left[e^{-i\sqrt{2}\cot(\frac{\theta}{2})Jt} \sin^2 \left(\frac{\theta}{2} \right) \right] \equiv \arg \left[e^{i\sqrt{2}\tan(\frac{\theta}{2})Jt} \cos^2 \left(\frac{\theta}{2} \right) \right] \equiv \arg(-1) \equiv \pi \pmod{2\pi}. \tag{C4}$$

Perfect state transfer occurs when $P_3^{(2)}(t) = 1$. Therefore, perfect state transfer occurs for angles θ_p and times τ_p that satisfy

$$\arg \left[e^{-i\sqrt{2}\cot\left(\frac{\theta_p}{2}\right)J\tau_p} \sin^2\left(\frac{\theta_p}{2}\right) \right] = -\sqrt{2}\cot\left(\frac{\theta_p}{2}\right)J\tau_p = 2p\pi + \pi, \quad (\text{C5})$$

for $p = -1, -2, -3, \dots$ [since $\cot\left(\frac{\theta}{2}\right) > 0$ for $0 < \theta < \pi$], and

$$\arg \left[e^{i\sqrt{2}\tan\left(\frac{\theta_p}{2}\right)J\tau_p} \cos^2\left(\frac{\theta_p}{2}\right) \right] = \sqrt{2}\tan\left(\frac{\theta_p}{2}\right)J\tau_p = 2m\pi + \pi, \quad (\text{C6})$$

for $m = 0, 1, 2, \dots$ [since $\tan\left(\frac{\theta}{2}\right) > 0$ for $0 < \theta < \pi$]. Dividing Eq. (C5) by Eq. (C6) gives

$$-\cot^2\left(\frac{\theta_p}{2}\right) = \frac{2p+1}{2m+1} \Rightarrow \cot^2\left(\frac{\theta_p}{2}\right) = \frac{-2p-1}{2m+1}. \quad (\text{C7})$$

If we let $n = -p - 1$, then

$$\cot^2\left(\frac{\theta_p}{2}\right) = \frac{2n+1}{2m+1}, \quad (\text{C8})$$

where $n, m = 0, 1, 2, \dots$, giving the condition in Eq. (16).

From Eq. (5), the corresponding detunings are given by

$$\begin{aligned} \Delta_p &= \frac{2\sqrt{2}J}{\tan\theta_p} = 2\sqrt{2}J \cot\theta_p = 2\sqrt{2}J \left[\frac{1}{2} \left(\cot\left(\frac{\theta_p}{2}\right) - \tan\left(\frac{\theta_p}{2}\right) \right) \right] \\ &= \sqrt{2}J \left(\frac{\sqrt{2n+1}}{\sqrt{2m+1}} - \frac{\sqrt{2m+1}}{\sqrt{2n+1}} \right) = \sqrt{2}J \left(\frac{2(n-m)}{\sqrt{2n+1}\sqrt{2m+1}} \right) = \frac{2\sqrt{2}J(n-m)}{\sqrt{2n+1}\sqrt{2m+1}}, \end{aligned} \quad (\text{C9})$$

giving the condition in Eq. (17).

From Eq. (C6), the times for perfect state transfer are given by

$$\tau_p = \frac{(2m+1)\pi}{\sqrt{2}J} \cot\left(\frac{\theta_p}{2}\right) = \frac{(2m+1)\pi}{\sqrt{2}J} \sqrt{\frac{2n+1}{2m+1}} = \frac{\pi\sqrt{(2n+1)(2m+1)}}{\sqrt{2}J}, \quad (\text{C10})$$

giving the condition in Eq. (18).

APPENDIX D: DERIVATION OF THE MAXIMAL NEGATIVITY CRITERION

Equations (B3a)–(B3c) can be written as

$$|\Psi_0\rangle = \sqrt{p_0}|\Phi_0\rangle, \quad |\Psi_1\rangle = \sqrt{p_1}|\Phi_1\rangle, \quad |\Psi_2\rangle = \sqrt{p_2}|\Phi_2\rangle, \quad (\text{D1})$$

where

$$p_0 = \langle\Psi_0|\Psi_0\rangle = (|a_1|^2 + |a_3|^2)^2, \quad (\text{D2a})$$

$$p_1 = \langle\Psi_1|\Psi_1\rangle = 2|a_2|^2(|a_1|^2 + |a_3|^2), \quad (\text{D2b})$$

$$p_2 = \langle\Psi_2|\Psi_2\rangle = |a_2|^4, \quad (\text{D2c})$$

and the normalized states $|\Phi_j\rangle$ are given by

$$|\Phi_0\rangle = \frac{1}{\sqrt{p_0}} \left(a_1^2|20\rangle + a_3^2|02\rangle + \sqrt{2}a_1a_3|11\rangle \right), \quad (\text{D3a})$$

$$|\Phi_1\rangle = \frac{1}{\sqrt{p_1}} \left(\sqrt{2}a_1a_2|10\rangle + \sqrt{2}a_2a_3|01\rangle \right), \quad (\text{D3b})$$

$$|\Phi_2\rangle = \frac{1}{\sqrt{p_2}} a_2^2|00\rangle. \quad (\text{D3c})$$

The reduced density matrix ρ_{13} can be written as a linear combination of density matrices as

$$\rho_{13} = \sum_{j=0}^2 p_j \rho_j, \quad (\text{D4})$$

where

$$\rho_0 = |\Phi_0\rangle\langle\Phi_0|, \quad \rho_1 = |\Phi_1\rangle\langle\Phi_1|, \quad \rho_2 = |\Phi_2\rangle\langle\Phi_2|. \tag{D5}$$

From the convexity of the negativity [23], we have

$$\mathcal{N}_{13} = \mathcal{N}(\rho_{13}) \leq \sum_{j=0}^2 p_j \mathcal{N}(\rho_j). \tag{D6}$$

The partial transpose of ρ_0 in the same basis used for $\rho_{13}^{T_3}$ is given by

$$\rho_0^{T_3} = \frac{1}{p_0} \begin{pmatrix} 0 & 0 & 0 & 0 & 0 & 0 & 0 & 0 & 0 & (a_1^* a_3)^2 \\ 0 & 0 & 0 & 0 & 0 & 0 & \sqrt{2} a_1^* a_3 |a_1|^2 & 0 & 0 & 0 \\ 0 & 0 & 0 & 0 & 0 & 0 & 0 & \sqrt{2} a_1^* a_3 |a_3|^2 & 0 & 0 \\ 0 & 0 & 0 & |a_1|^4 & 0 & 0 & 0 & 0 & 0 & 0 \\ 0 & 0 & 0 & 0 & 2|a_1 a_3|^2 & 0 & 0 & 0 & 0 & 0 \\ 0 & 0 & 0 & 0 & 0 & |a_3|^4 & 0 & 0 & 0 & 0 \\ 0 & \sqrt{2} a_1 a_3^* |a_1|^2 & 0 & 0 & 0 & 0 & 0 & 0 & 0 & 0 \\ 0 & 0 & \sqrt{2} a_1 a_3^* |a_3|^2 & 0 & 0 & 0 & 0 & 0 & 0 & 0 \\ (a_1 a_3^*)^2 & 0 & 0 & 0 & 0 & 0 & 0 & 0 & 0 & 0 \end{pmatrix}. \tag{D7}$$

The eigenvalues of this matrix are $\frac{1}{p_0} |a_1|^4$, $\frac{1}{p_0} |a_3|^4$, $\pm \frac{1}{p_0} |a_1 a_3|^2$, $\frac{2}{p_0} |a_1 a_3|^2$, $\pm \frac{\sqrt{2}}{p_0} |a_1|^3 |a_3|$, and $\pm \frac{\sqrt{2}}{p_0} |a_1| |a_3|^3$. Therefore, using the negative (or possibly zero) eigenvalues, the negativity for ρ_0 is

$$\mathcal{N}(\rho_0) = \frac{1}{p_0} [|a_1 a_3|^2 + \sqrt{2} |a_1 a_3| (|a_1|^2 + |a_3|^2)]. \tag{D8}$$

Next, the partial transpose of ρ_1 in the same basis as above is given by

$$\rho_1^{T_3} = \frac{1}{p_1} \begin{pmatrix} 0 & 0 & 0 & 0 & 2a_1^* a_3 |a_2|^2 & 0 & 0 & 0 & 0 \\ 0 & 2|a_1 a_2|^2 & 0 & 0 & 0 & 0 & 0 & 0 & 0 \\ 0 & 0 & 2|a_2 a_3|^2 & 0 & 0 & 0 & 0 & 0 & 0 \\ 0 & 0 & 0 & 0 & 0 & 0 & 0 & 0 & 0 \\ 2a_1 a_3^* |a_2|^2 & 0 & 0 & 0 & 0 & 0 & 0 & 0 & 0 \\ 0 & 0 & 0 & 0 & 0 & 0 & 0 & 0 & 0 \\ 0 & 0 & 0 & 0 & 0 & 0 & 0 & 0 & 0 \\ 0 & 0 & 0 & 0 & 0 & 0 & 0 & 0 & 0 \\ 0 & 0 & 0 & 0 & 0 & 0 & 0 & 0 & 0 \end{pmatrix}. \tag{D9}$$

The eigenvalues of this matrix are 0 (repeated five times), $\frac{2}{p_1} |a_1 a_2|^2$, $\frac{2}{p_1} |a_2 a_3|^2$, and $\pm \frac{2}{p_1} |a_1 a_3| |a_2|^2$. Therefore, using the negative (or possibly zero) eigenvalue and the relation $|a_1|^2 + |a_2|^2 + |a_3|^2 = 1$, the negativity for ρ_1 is

$$\mathcal{N}(\rho_1) = \frac{2}{p_1} |a_1 a_3| |a_2|^2 = \frac{2}{p_1} |a_1 a_3| (1 - |a_1|^2 - |a_3|^2). \tag{D10}$$

Finally, the partial transpose of ρ_2 in the same basis as above is given by

$$\rho_2^{T_3} = \frac{1}{p_2} \begin{pmatrix} |a_2|^4 & 0 & 0 & 0 & 0 & 0 & 0 & 0 & 0 \\ 0 & 0 & 0 & 0 & 0 & 0 & 0 & 0 & 0 \\ 0 & 0 & 0 & 0 & 0 & 0 & 0 & 0 & 0 \\ 0 & 0 & 0 & 0 & 0 & 0 & 0 & 0 & 0 \\ 0 & 0 & 0 & 0 & 0 & 0 & 0 & 0 & 0 \\ 0 & 0 & 0 & 0 & 0 & 0 & 0 & 0 & 0 \\ 0 & 0 & 0 & 0 & 0 & 0 & 0 & 0 & 0 \\ 0 & 0 & 0 & 0 & 0 & 0 & 0 & 0 & 0 \\ 0 & 0 & 0 & 0 & 0 & 0 & 0 & 0 & 0 \end{pmatrix}. \tag{D11}$$

The eigenvalues of this matrix are 0 (repeated eight times) and $\frac{1}{p_2} |a_2|^4$. Since the matrix has no negative eigenvalues, we have

$$\mathcal{N}(\rho_2) = 0. \tag{D12}$$

Using Eqs. (D8), (D10), and (D12), Eq. (D6) becomes

$$\mathcal{N}_{13} \leq |a_1 a_3|^2 + \sqrt{2} |a_1 a_3| (|a_1|^2 + |a_3|^2) + 2 |a_1 a_3| (1 - |a_1|^2 - |a_3|^2). \tag{D13}$$

Now,

$$0 \leq (|a_1| - |a_3|)^2 = |a_1|^2 + |a_3|^2 - 2|a_1 a_3| \Rightarrow |a_1 a_3| \leq \frac{1}{2}(|a_1|^2 + |a_3|^2), \quad (\text{D14})$$

with equality when $|a_1| = |a_3|$. Therefore,

$$\begin{aligned} \mathcal{N}_{13} &\leq \left[\frac{1}{2}(|a_1|^2 + |a_3|^2) \right]^2 + \frac{1}{\sqrt{2}}(|a_1|^2 + |a_3|^2)(|a_1|^2 + |a_3|^2) + (|a_1|^2 + |a_3|^2)(1 - |a_1|^2 - |a_2|^2) \\ &= \frac{1}{4}(|a_1|^2 + |a_3|^2)[(2\sqrt{2} - 3)(|a_1|^2 + |a_3|^2) + 4]. \end{aligned} \quad (\text{D15})$$

Since $0 \leq |a_1|^2 + |a_3|^2 = 1 - |a_2|^2 \leq 1$ and $\frac{1}{4}x[(2\sqrt{2} - 3)x + 4]$ is an increasing function of x for $0 \leq x \leq 1$, we have

$$\mathcal{N}_{13} \leq \frac{1}{4} + \frac{1}{\sqrt{2}}, \quad (\text{D16})$$

with equality when $|a_1| = |a_3|$ and $|a_1|^2 + |a_3|^2 = 1$. In this case, $|a_1| = |a_3| = \frac{1}{\sqrt{2}}$ and $|a_2| = 0$. Using Eq. (8b), the maximum negativity occurs for angles θ_N and times τ_N that satisfy

$$\begin{aligned} |a_2| &= \left| \frac{1}{2\sqrt{2}} \left(e^{-i\sqrt{2} \cot(\frac{\theta_N}{2}) J \tau_N} - e^{i\sqrt{2} \tan(\frac{\theta_N}{2}) J \tau_N} \right) \sin \theta_N \right| = 0 \\ &\Rightarrow \left| e^{-i\sqrt{2} \cot(\frac{\theta_N}{2}) J \tau_N} - e^{i\sqrt{2} \tan(\frac{\theta_N}{2}) J \tau_N} \right| = 0 \\ &\Rightarrow e^{-i\sqrt{2} \cot(\frac{\theta_N}{2}) J \tau_N} = e^{i\sqrt{2} \tan(\frac{\theta_N}{2}) J \tau_N}. \end{aligned} \quad (\text{D17})$$

Using Eqs. (8a) and (D17), we have

$$\begin{aligned} |a_1| &= \left| \frac{1}{2} \left[e^{i\sqrt{2} \tan(\frac{\theta_N}{2}) J \tau_N} \sin^2 \left(\frac{\theta_N}{2} \right) + e^{i\sqrt{2} \tan(\frac{\theta_N}{2}) J \tau_N} \cos^2 \left(\frac{\theta_N}{2} \right) + 1 \right] \right| = \frac{1}{\sqrt{2}} \\ &\Rightarrow \left| e^{i\sqrt{2} \tan(\frac{\theta_N}{2}) J \tau_N} \left[\sin^2 \left(\frac{\theta_N}{2} \right) + \cos^2 \left(\frac{\theta_N}{2} \right) \right] + 1 \right|^2 = 2 \\ &\Rightarrow \left| e^{i\sqrt{2} \tan(\frac{\theta_N}{2}) J \tau_N} + 1 \right|^2 = 2 \\ &\Rightarrow e^{i\sqrt{2} \tan(\frac{\theta_N}{2}) J \tau_N} + e^{-i\sqrt{2} \tan(\frac{\theta_N}{2}) J \tau_N} + 2 = 2 \\ &\Rightarrow e^{i\sqrt{2} \tan(\frac{\theta_N}{2}) J \tau_N} = e^{-i\sqrt{2} \tan(\frac{\theta_N}{2}) J \tau_N + i\pi} \\ &\Rightarrow \sqrt{2} \tan \left(\frac{\theta_N}{2} \right) J \tau_N = -\sqrt{2} \tan \left(\frac{\theta_N}{2} \right) J \tau_N + \pi + 2m\pi \\ &\Rightarrow 2\sqrt{2} \tan \left(\frac{\theta_N}{2} \right) J \tau_N = (2m + 1)\pi, \end{aligned} \quad (\text{D18})$$

where $m = 0, 1, 2, \dots$. From Eq. (D17), we have

$$\begin{aligned} -\sqrt{2} \cot \left(\frac{\theta_N}{2} \right) J \tau_N &= \sqrt{2} \tan \left(\frac{\theta_N}{2} \right) J \tau_N + 2p\pi \\ \Rightarrow -2\sqrt{2} \cot \left(\frac{\theta_N}{2} \right) J \tau_N &= 2\sqrt{2} \tan \left(\frac{\theta_N}{2} \right) J \tau_N + 4p\pi \\ &= (2m + 4p + 1)\pi \end{aligned} \quad (\text{D19})$$

for integers p such that $2m + 4p + 1 < 0$, since $\cot(\frac{\theta}{2}) > 0$. Dividing Eq. (D19) by Eq. (D18) gives

$$-\cot^2 \left(\frac{\theta_N}{2} \right) = \frac{2m + 4p + 1}{2m + 1} \Rightarrow \cot^2 \left(\frac{\theta_N}{2} \right) = \frac{-2m - 4p - 1}{2m + 1} = \frac{2n + 1}{2m + 1}, \quad (\text{D20})$$

where $n = -m - 2p - 1$. Since $2m + 4p + 1 < 0$, we have $n = -m - 2p - 1 > -\frac{1}{2}$ and so $n = 0, 1, 2, \dots$. Also, $n - m = -2(m + p) + 1$, which is odd. Therefore, the maximum negativity occurs for angles θ_N that satisfy Eq. (16), with the added constraint that $(n - m)$ is odd. It follows that the maximum negativity occurs for detunings that satisfy Eq. (17), with the

constraint that $(n - m)$ is odd. From Eq. (D18), the maximum negativity occurs at times τ_N that satisfy

$$\tau_N = \frac{(2m + 1)\pi}{2\sqrt{2}J} \cot\left(\frac{\theta_N}{2}\right) = \frac{(2m + 1)\pi}{2\sqrt{2}J} \sqrt{\frac{2n + 1}{2m + 1}} = \frac{\pi\sqrt{(2n + 1)(2m + 1)}}{2\sqrt{2}J}, \quad (\text{D21})$$

with the constraint that $(n - m)$ is odd.

-
- [1] J. P. Dowling and G. J. Milburn, Quantum technology: The second quantum revolution, *Philos. Trans. R. Soc. A* **361**, 1655 (2003).
- [2] C. A. Fuchs, Quantum mechanics as quantum information, mostly, *J. Mod. Opt.* **50**, 987 (2003).
- [3] C. Bengtson and E. Sjöqvist, The role of quantum coherence in dimer and trimer excitation energy transfer, *New J. Phys.* **19**, 113015 (2017).
- [4] E. Wyke, A. Aiyejina, and R. Andrews, Quantum excitation transfer, entanglement, and coherence in a trimer of two-level systems at finite temperature, *Phys. Rev. A* **101**, 062101 (2020).
- [5] M. Christandl, N. Datta, A. Ekert, and A. J. Landahl, Perfect State Transfer in Quantum Spin Networks, *Phys. Rev. Lett.* **92**, 187902 (2004).
- [6] J. Q. You and F. Nori, Atomic physics and quantum optics using superconducting circuits, *Nature (London)* **474**, 589 (2011).
- [7] N. Goss, A. Morvan, B. Marinelli, B. K. Mitchell, L. B. Nguyen, R. K. Naik, L. Chen, C. Jünger, J. M. Kreikebaum, D. I. Santiago, J. J. Wallman, and I. Siddiqi, High-fidelity qutrit entangling gates for superconducting circuits, *Nat. Commun.* **13**, 7481 (2022).
- [8] K. Luo, W. Huang, Z. Tao, L. Zhang, Y. Zhou, J. Chu, W. Liu, B. Wang, J. Cui, S. Liu, F. Yan, M.-H. Yung, Y. Chen, T. Yan, and D. Yu, Experimental Realization of Two Qutrits Gate with Tunable Coupling in Superconducting Circuits, *Phys. Rev. Lett.* **130**, 030603 (2023).
- [9] M. Fleischhauer, A. Imamoglu, and J. P. Marangos, Electromagnetically induced transparency: Optics in coherent media, *Rev. Mod. Phys.* **77**, 633 (2005).
- [10] S. H. Autler and C. H. Townes, Stark effect in rapidly varying fields, *Phys. Rev.* **100**, 703 (1955).
- [11] N. V. Vitanov, A. A. Rangelov, B. W. Shore, and K. Bergmann, Stimulated Raman adiabatic passage in physics, chemistry, and beyond, *Rev. Mod. Phys.* **89**, 015006 (2017).
- [12] A. D. Greentree, S. G. Schirmer, F. Green, L. C. L. Hollenberg, A. R. Hamilton, and R. G. Clark, Maximizing the Hilbert Space for a Finite Number of Distinguishable Quantum States, *Phys. Rev. Lett.* **92**, 097901 (2004).
- [13] H. J. Bernstein, Superdense quantum teleportation, *Quantum Inf. Proc.* **5**, 451 (2006).
- [14] B. P. Lanyon, M. Barbieri, M. P. Almeida, T. Jennewein, T. C. Ralph, K. J. Resch, G. J. Pryde, J. L. O'Brien, A. Gilchrist, and A. G. White, Simplifying quantum logic using higher-dimensional Hilbert spaces, *Nat. Phys.* **5**, 134 (2009).
- [15] E. T. Campbell, Enhanced Fault-Tolerant Quantum Computing in d -Level Systems, *Phys. Rev. Lett.* **113**, 230501 (2014).
- [16] P. Gokhale, J. M. Baker, C. Duckering, N. C. Brown, K. R. Brown, and F. T. Chong, Asymptotic improvements to quantum circuits via qutrits, in *Proceedings of the 46th International Symposium on Computer Architecture, ISCA '19* (Association for Computing Machinery, New York, NY, 2019), pp. 554–566.
- [17] N. J. Cerf, M. Bourennane, A. Karlsson, and N. Gisin, Security of Quantum Key Distribution Using d -Level Systems, *Phys. Rev. Lett.* **88**, 127902 (2002).
- [18] Y.-H. Luo, H.-S. Zhong, M. Erhard, X.-L. Wang, L.-C. Peng, M. Krenn, X. Jiang, L. Li, N.-L. Liu, C.-Y. Lu, A. Zeilinger, and J.-W. Pan, Quantum Teleportation in High Dimensions, *Phys. Rev. Lett.* **123**, 070505 (2019).
- [19] C. Senko, P. Richerme, J. Smith, A. Lee, I. Cohen, A. Retzker, and C. Monroe, Realization of a Quantum Integer-Spin Chain with Controllable Interactions, *Phys. Rev. X* **5**, 021026 (2015).
- [20] A. D. Greentree and B. Koiller, Dark-state adiabatic passage with spin-one particles, *Phys. Rev. A* **90**, 012319 (2014).
- [21] A. Aiyejina, E. Wyke, and R. Andrews, Near-Perfect Two-Photon State Transfer in a Trimer of Three-Level Systems, in *Frontiers in Optics + Laser Science 2022 (FIO, LS)*, edited by R. Bartels and D. Reis (Optica, Washington, DC, 2022), p. JW4B.13.
- [22] O. Civitarese, M. Reboiro, L. Rebón, and D. Tielas, Atomic squeezing in three-level atoms with effective dipole-dipole atomic interaction, *Phys. Lett. A* **374**, 2117 (2010).
- [23] G. Vidal and R. F. Werner, Computable measure of entanglement, *Phys. Rev. A* **65**, 032314 (2002).